Journal of Clinical and Medical Images

Research Article

ISSN: 2640-9615 | Volume 7

Preliminary Study on Monitoring Drug Resistance of Colon Cancer with Intravoxel Incoherent Motion MRI in Vivo

Xie Q[1*], Yang YM[2], Wang GQ[3], Wu MY[4], Zhang J[5] and Wu JB[1]

[1]Medical Imaging Department, Nansha Branch of Guangzhou First People's Hospital, School of Medicine, South China University of Technology, China

[2]Department of Radiology, Guangdong Provincial Hospital of Traditional Chinese Medicine, Guangzhou University of Traditional Chinese Medicine, China

[3]Medical Record Department, Nansha Branch of Guangzhou First People's Hospital, School of Medicine, South China University of Technology, China

[4]Department of Radiology, Panyu central Hospital of Guangzhou, China

[5]Department of Pathology, Cancer Center, Sun Yat-sen University, China

[*]Corresponding author:

Qi Xie,
Medical Imaging Department, Nansha Branch of Guangzhou First People's Hospital, School of Medicine, South China University of Technology, No. 105, Fengzedong Road, Guangzhou 511457, Canton, China

Received: 07 Oct 2023
Accepted: 08 Nov 2023
Published: 17 Nov 2023
J Short Name: JCMI

Keywords:

Intravoxel incoherent motion (IVIM); Magnetic resonance imaging (MRI); Xenograft model in nude mice; Human colon cancer; Multiple drug resistance

Citation:

Xie Q, Preliminary Study on Monitoring Drug Resistance of Colon Cancer with Intravoxel Incoherent Motion MRI in Vivo. J Clin Med Img. 2023; V7(6): 1-8

1. Abstract

1.1. Introduction: The current study investigated the role of intravoxel incoherent motion-DWI (IVIM-DWI) in evaluating drug resistance in colon cancer xenografts and explored possible biomarkers.

1.2. Methods: Ten healthy BALB/c nude mice were randomly divided into 2 groups (5 each) and injected with SW480 or SW480/5-fluorouracil (5-FU) cell suspensions. IVIM-DWI was performed when the long-axis diameter of the tumour was close to 1.5 centimetres. Then, tumours were removed to detect the protein expression of permeability glycoprotein (P-gp, MDR), multidrug resistance associated protein 1 (MRP1) and protein kinase C (PKC), cell morphology, necrosis and drug resistance.

1.3. Results: The apparent diffusion coefficient (ADC), D and D* values were significantly higher in the SW480 group than in the SW480/5-FU group (p: 0.001, 0.002, 0.037), and ADC and D values were negatively correlated with the expression of tumour drug resistance-associated proteins, including P-gp, MRP1, and PKC (p: 0.006, 0.007, 0.022). There were no significant differences in the f values between the two groups. The cell nuclei were larger, and the cells were arranged more closely in the SW480/5-FU group. The degree of tumour necrosis was not significantly different between the two groups. The protein expression of P-gp, MRP1, and PKC was significantly higher in the SW480/5-FU group ($p<0.05$).

1.4. Conclusion: The ADC value of DWI and the D and D*values of IVIM were of moderate value for discriminating between 5-FU-responsive and 5-FU-resistant colon cancers in vivo. This may become a potential imaging biomarker for the in vivo monitoring of tumour drug resistance.

2. Introduction

Currently, palliative chemotherapy with 5-fluorouracil (5-FU)-based therapy is the most common therapy for patients with advanced colorectal cancer (CRC) [1]. Unfortunately, the progression-free survival period is only 8.7 to 12.3 months [2] because of the development of CRC drug resistance during treatment [3]. It is of great significance to monitor drug resistance in CRC in a timely

and accurate manner during treatment. At present, an in vitro drug susceptibility test that is invasive and time-consuming is used to evaluate drug resistance.

During the development of drug resistance in cancer cells, changes in the microstructure and microcirculation in tumour tissues, as well as metabolites related to tumour resistance, may cause changes in the tumour microenvironment [4].

As a relatively new technical improvement in magnetic resonance imaging (MRI), diffusion-weighted imaging (DWI), including single-exponential-model DWI and multiple-b-value intravoxel incoherent motion (IVIM) [5-6], can be used to assess the diffusion of water molecules (Brownian motion) into biological tissues [5]. Studies have shown that the degree of water diffusion limitation in biological tissue is inversely correlated with cell density and cell membrane integrity [5]. Therefore, DWI can be used to visualize relevant information on the microenvironment of biological tissue in vivo. As a multib-value diffusion image analysis technique, IVIM can noninvasively separate pure water molecular diffusion and capillary perfusion, reflecting the perfusion and diffusion characteristics of tissues [6]. It is more advantageous to display the microscopic characteristics of biological tissues in vivo.

Much work has been done based on MR-DWI and has provided quantitative parameters, including the apparent diffusion coefficient (ADC) and IVIM parameters (D, pure diffusion; f, perfusion fraction; and D*, pseudodiffusion). In recent years, most research interests have focused on developing various MR-DWI-derived parameters, exploring the role of these parameters in evaluating tumour biological features, predicting tumour invasiveness, monitoring the treatment response, predicting tumour prognosis, and distinguishing between malignant and benign lymph nodes [7-13]. MR-DWI in the evaluation of drug resistance in tumours has rarely been investigated.

Previously, we reported that the ADC values of 5-FU-responsive colon cancer tissue in xenografts were higher than those of 5-FU-resistant tissue by using monoexponential model DWI detection with 1.5 T MRI [14-15]. Therefore, we hypothesized that DWI has potential feasibility for detecting tumour resistance in vivo [14-15]. In the present study, 3.0 T MRI was used to further analyse 5-FU-responsive and 5-FU-resistant colon cancer tissue using IVIM techniques from preclinical models. We aimed to investigate whether IVIM with multiple b values can be used to accurately visualize the microenvironment of tumour tissue, including characteristic subtle changes in tumour perfusion and diffusion between 5-FU-responsive tissue and 5-FU-resistant colon cancer tissue in vivo. We also explored whether IVIM parameters could be used to monitor drug resistance in tumours in vivo and the corresponding histopathology and molecular mechanisms.

3. Methods

3.1. Animal Models

The human CRC parental cell line SW480 and BALB/c nude mice were purchased from the Experimental Animal Center of Sun Yat-sen University (No. 44007200046136, Guangzhou, China). All experimental protocols were approved by the Ethical Committee for Animal Research of Guangzhou Medical University (GY2017-007).

The drug-resistant SW480 cell line was induced by the high-dose impact method [16]. The SW480 cell line was cultured in RPMI 1640 medium (HyClone Laboratories, Logan, UT, United States) supplemented with 10% foetal bovine serum (Gibco, Invitrogen, Waltham, MA, United States) and 100 U/mL penicillin (Solarbio Life Science, Beijing, China) at 37°C in a humidified 5% CO2 atmosphere. These cells in logarithmic growth phase were cultured in medium containing 6 μg/ml 5-FU for 24 hours, and then the medium was replaced with RPMI 1640 medium twice a day. When the cells resumed the logarithmic growth phase, they were cultured in medium containing 6 μg/ml 5-FU for 24 hours again. After continuous alternating cultivation for 6 months, the cell line that was able to grow in medium containing 6 μg/ml 5-FU was obtained and designated SW480/5-FU.

Ten healthy female BALB/c nude mice, 5-6 weeks old and weighing 16-18 g, were randomly divided into a resistant group and a responsive group (5 each). SW480/5-FU or SW480 cell suspensions (0.2 ml, cell concentration 4×107/ml) were injected into the bilateral hind leg root, and then the animals were housed in the specific pathogen-free facility of the Animal Experimental Center of Guangzhou Medical University. Based on the ethical standard of tumour burden on mice in the «Guidelines for the welfare and use of animals in cancer research, 2010» [17], the maximal diameter of tumours in mice was limited to less than 15 mm. Eight tumours with the largest diameter close to 15mm were examined by MRI.

3.2. MRI and Analysis

Before the MR examination, each mouse was wrapped with a plastic outer coating to keep warm and prevent curling artefacts.

MRI was performed using a MAGNETOM Skyro 3.0 T clinical scanner (Siemens, Germany) with an 8-channel mouse coil (Chenguang Medical Technology Co., Shanghai, China). T2-weighted turbo spin–echo (TSE) images and IVIM sequences were obtained for all mice. The main scanning parameters of the MR sequences were as follows.

T2-weighted imaging (T2WI): TR/TE=4500 ms/110 ms, slice thickness=2 mm, interval=0, FOV=128 mm, matrix=128×128.

IVIM-DWI: Axial imaging was performed with single-shot echo-planar imaging (EPI), an isotropic diffusion-sensitive gradient field, 8 b values (0, 10, 20, 30, 40, 50, 100, 150, 200, 400,

600, and 800 s/mm2), TR=3400 ms, TE=60 ms, FOV=220 mm, NAS=4, slice thickness=2 mm, acquisition matrix=220×220.

Multi-b value DWI data were analysed with MITK Diffusion (German Cancer Research Center, MITK diffusion, Version 2013.03.00) and bi-exponential decay fitting (segmented fitting with threshold of 200 b values) for Xenograft model intravoxel incoherent motion diffusion MRI. The regions of interest (ROIs) were manually drawn in the largest section of the tumour, avoiding bleeding and cystic and necrotic areas, by two radiologists (Yang & Wu) independently who were blinded to tumour-related information. Each tumour was measured three times by each radiologist. The average value measured by the two radiologists was included in the analysis. The acquisition parameters included the ADC, D, D* and f values of the tumour.

The mean ROI size was 51.1 mm2 (range, 7.1–94.91 mm2) by observer 1 and 52.3 mm2 (range, 8.4–98.2 mm2) by observer 2.

3.3. Experimental Evaluation of Specimens

The tumour-bearing mice were intraperitoneally injected with 1-2 ml 4% chloral hydrate after the MR examination. The tumours were excised and divided into three portions (one for Western blotting, another for haematoxylin-eosin (HE) staining, and another for MTT assays).

3.4. Western Blotting

Western blotting was conducted by Getway Biotechnology Co., Ltd. (Guangzhou, China). Permeability glycoprotein (P-gp, MDR), multidrug resistance-associated protein 1 (MRP1) and protein kinase C (PKC) were detected following the instruction manual for the Phototope®-HRP Western blot Kit (Cell Signaling Technology, Danvers, MA, United States). Antibodies (ABclonal, Wuhan, China) included goat anti-mouse IgG/HRP (AS003, 1:5000 dilution), P-gp (A11758, 1:1000 dilution), MRP1 (A3027, 1:1000 dilution), PKC (A0267, 1:1000 dilution) and GAPDH (AC001, 1:1000 dilution).

The abovementioned protein bands were scanned into a computer in JPG format, and the integrated optical density (IOD) of band intensity was obtained using Image-Pro Plus 6.0 software. The IOD of protein expression was divided by the IOD of the internal reference (GAPDH) to obtain the relative IOD (RIOD) of each protein.

3.5. HE Staining

The pathological sections were evaluated by a pathologist with 30 years of work experience (Zhang J). Tumour necrosis was assessed in HE-stained sections (magnification ×400) as follows: The degree of necrosis was rated on a scale from 0~5 points as follows: 1 point (light), tumour necrosis accounted for approximately 1/5 of the tumour tissue; 2 points (moderate), tumour necrosis accounted for approximately 2/5 of the tumour tissue; 3 points (severe), tumour necrosis accounted for approximately 3/5 of the tumour tissue; 4 points (very severe), tumour necrosis accounted for approximately 4/5 of the tumour tissue; and 5 points, total tumour necrosis. The necrotic area is extremely small at 0.5 points.

3.6. In vitro drug sensitivity test for detecting 5-FU resistance in colon cancer xenografts

The sensitivity of CRC cells to 5-FU was assessed using the MTT assay as described previously [18]. Briefly, tumour tissues were cut into small pieces (approximately 1 to 2 mm3 in size) and placed into EP tubes. Next, 1 ml trypsin-EDTA (Gibco, Invitrogen, Waltham, MA, United States) was added for digestion for 50 min in a 37°C incubator, 2 ml RPMI 1640 medium (HyClone Laboratories, Logan, UT, United States) was added to terminate digestion, the suspension was aspirated into a 15 ml centrifuge tube and centrifuged for 5 min (rotation speed 1000 r/min), the supernatant was discarded, 2~3 ml RPMI 1640 medium filtered through a 200-mesh sieve was added, and the cell suspension was placed in a 25 cm2 culture flask. The half-maximal inhibitory concentration (IC50) values of SW480/5-FU and SW480 xenograft tumours were measured with MTT assays.

3.7. Statistical Analyses

The SPSS 13.1 statistical package (SPSS, Chicago, USA) was used for all the calculations. Continuous variables are shown as the mean±standard deviation (SD). The results of the normality test (Kolmogorov–Smirnov test) showed that IVIM parameters conformed to a normal distribution. Two-sample T tests were used to compare the degree of necrosis and IVIM parameters between the 5-FU-responsive group and the 5-FU-resistant group. The Mann–Whitney U test was used to compare the protein expression of P-gp, PKC and MRP1 between the two groups. The correlation between IVIM parameters and the protein expression of P-gp, PKC and MRP1 was determined by the Spearman correlation test. $p< 0.05$ was considered statistically significant.

The intraclass correlation coefficient (ICC) was used to assess the interobserver differences in IVIM parameter measurements. The ratings were considered poor (ICC<0.40), moderate (ICC=0.40-0.59), good (ICC=0.60-0.74) or excellent (ICC=0.75-1.00).

4. Results

4.1. Pathological features of SW480 and SW480/5-FU colorectal tumours

The degree of tumour necrosis was 1.33±0.58 points and 1.50±0.50 points in the SW480 and SW480/5-FU groups, respectively, without a statistically significant difference ($p>0.05$). The cell nuclei were significantly larger and the cells were arranged more closely with smaller cell gaps in the SW480/5-FU group than in the SW480 group (Figure 1).

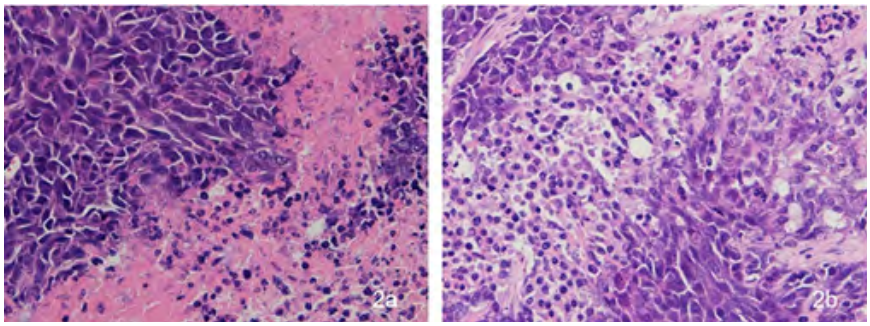

Figure 1: HE sections of SW480/5-FU cells (2a,400 ×) and SW480 cells (2b,400 ×). The cell nucleus was larger and arranged more closely in SW480/5-FU group than in SW480 group.

4.2. In vitro susceptibility test for detecting 5-FU resistance in SW480 and SW480/5-FU xenografts

The IC50 values of SW480/5-FU and SW480 xenografts were 42.9 μg/ml and 9.516 μg/ml, respectively, as determined with MTT assays (RI=4.508).

The cell survival rate of SW480/5-FU and SW480 cancer tissues decreased with increasing 5-FU concentrations. However, the SW480/5-FU tumour tissues had a significantly higher cell survival rate than the SW480 tumour tissues when the 5-FU concentration was smaller than 50 μg/ml ($p<0.05$) (Figure 2). The SW480/5-FU tumour cells were resistant to 5-FU at 5-U concentrations below 50 μg/ml.

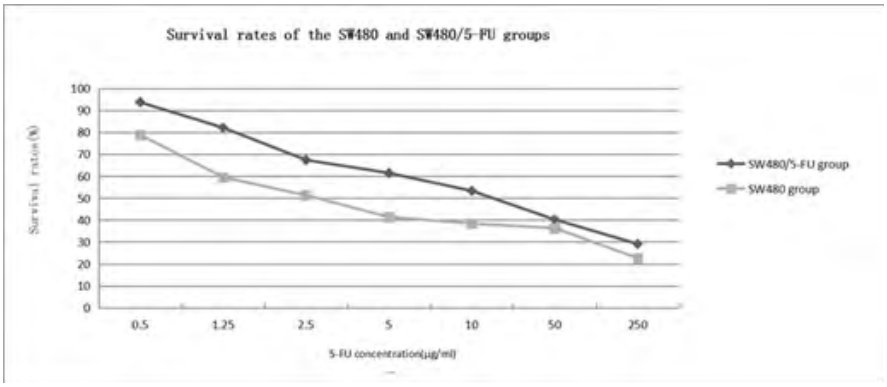

Figure 2: Survival rates of SW480/5-FU and SW480 cells at different concentrations of 5-FU.

4.3. Expression of P-gp, MRP1 and PKC in SW480/5-FU and SW480 xenografts by Western blotting

The expression of P-gp, MRP1 and PKC was higher in SW480/5-FU xenografts than in SW480 xenografts (Figure 3).

The RIOD values of the expression levels of these proteins were significantly different between the two groups ($p<0.01$, Table 1). The expression levels of drug resistance-associated proteins suggested that SW480/5-FU cancer cells were resistant to 5-FU.

Table 1: The RIOD values of P-gp, MRP1 and PKC for SW480/5-FU and SW480 ($\bar{x}$±s)

group (n=8)	P-gp	MRP1	PKC
SW480	0.20±0.03	0.15±0.01	0.16±0.02
SW480/5-FU	0.31±0.08	0.69±0.10	0.86±0.06
Z	2.611	2.785	2.668
p	0.003	0.005	0.008

Mann- Whitney U test was used for compare the protein expression of P-gp, PKC and MRP1 between 5-FU- responsive and 5-FU-resistant group

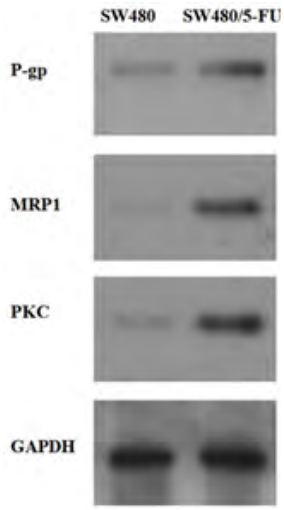

Figure 3: The expression of P-gp, MRP1 and PKC in SW480/5-FU and SW480 colon cancer cells.

4.4. IVIM parameters and ADC values of SW480/5-FU and SW480 xenografts

4.4.1. Interobserver agreement: The interobserver differences in IVIM parameters (assessed by the ICC) are listed in Table 2. The ICCs of the ADC, D, D* and f values were 0.788, 0.845, 0.805 and 0.770, respectively. Excellent data agreement was reached between observers.

4.5. ADC values and IVIM parameters of SW480/5-FU and SW480 xenografts

Parametric maps of the ADC, D, D* and f values of the SW480/5-FU and SW480 xenografts are shown in Figure 4. Compared with the mass of SW480 cells, the mass of SW480/5-FU cells showed signal attenuation on the ADC, D and D*parameter map of IVIM DWI. Visually, ADC, D and D* decreased in drug-resistant tissues.

The ADC, D, D* and f values of the SW480/5-FU and SW480 xenografts are summarized in Table 3 and Figure 5. The ADC, D and D* values of the SW480/5-FU xenografts were significantly lower than those of the SW480 xenografts (p: 0.001, 0.002, 0.037). The f values tended to be lower in SW480/5-FU xenografts than in SW480 xenografts, but the difference was not statistically significant (p =0.091, Table 3).

Table 2: Intraclass correlation coefficient (ICC) of parameter measurements between two observers

Parameter	ADC	D	D*	*f*
ICC	0.788	0.845	0.805	0.77
95 % CI	35.3%-94.3%	49.5%-95.9%	39.5%-94.8%	31.3%-93.7%

CI: confidence interval.

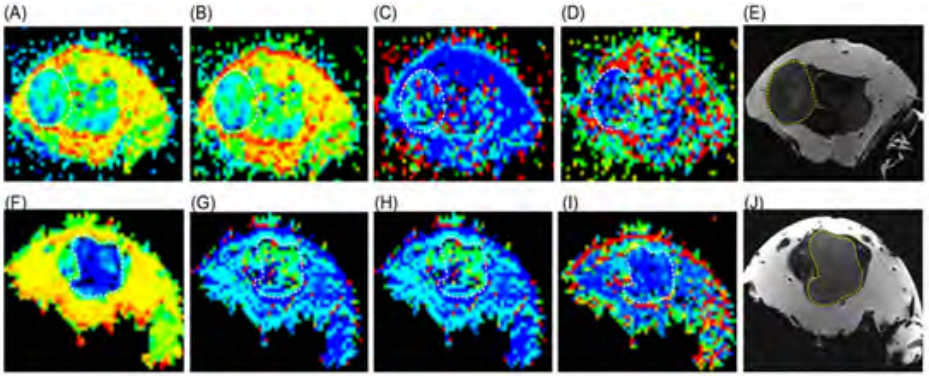

Figure 4: IVIM DWI parametric maps of ADC, D, D* and f values and T2W images for SW480 (A-E) and SW480/5-FU (F-J) cells.

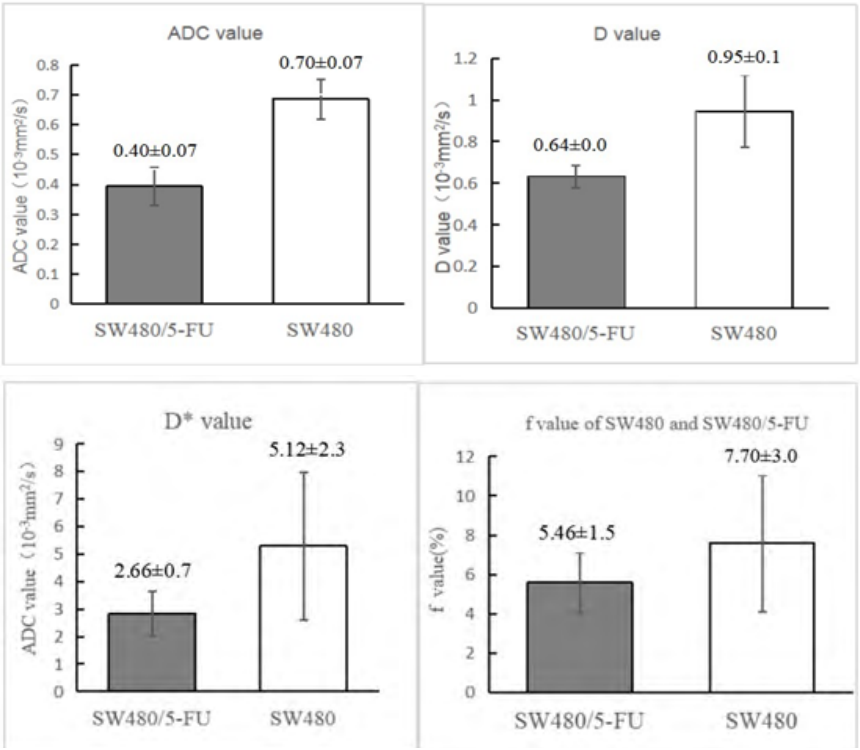

Figure 5: The Comparison of the ADC, D, D* and f values between SW480/5-FU and SW480 xenografts.

Table 3: The mean ADC, D, D*, and f values of SW480/5-FU and SW480 xenografts ($\bar{x}$±s)

group (n=8)	ADC ($10^{-3}mm^2/s$)	D ($10^{-3}mm^2/s$)	D* ($10^{-3}mm^2/s$)	*f*(%)
SW480/5-FU	0.40±0.07	0.64±0.05	2.66±0.73	5.46±1.53
SW480	0.70±0.07	0.95±0.18	5.12±2.33	7.70±3.03
t	8.54	4.704	2.48	1.86
p	0.001	0.002	0.037	0.091

Two-sample T test was used for comparison parameters (ADC,D,D* and f) between 5-FU-responsive and 5-FU-resistant group.

4.6. Correlation between IVIM and the expression of P-gp, MRP1, and PKC in CRC (Spearman correlation test)

The ADC values of CRC tissues were negatively correlated with their expression of P-gp (r: -0.794, p: 0.006), MRP1 (r: -0.769, p: 0.007) and PKC (r: -0.706, p: 0.022). The D values of CRC tissues were negatively correlated with their expression of P-gp (r: -0.70, p: 0.03), MRP1 (r: -0.93, p: 0.00) and PKC (r: -0.69, p: 0.03).

5. Discussion

This study showed that the ADC, D and D* values of the SW480/5-FU xenografts were significantly lower than those of the SW480 xenografts. Next, the scientific basis and potential value of the findings of this study are discussed from the pathophysiological mechanism of tumour drug resistance, the reliability of the drug resistance model in this study, and the principle and application status of IVIM-DWI.

Cancer cell resistance can be intrinsic or acquired through exposure to certain chemotherapeutic compounds [19-20]. Cancer cells can become resistant to many compounds via different mechanisms [21], which is known as multidrug resistance (MDR). MDR may be related to many different biochemical processes [22].

In cancer cells with MDR, the ATP binding cassette (ABC) transporter is highly expressed. This transporter actively effluxes the transport of chemotherapeutic drugs to reduce the intracellular concentration of drugs and metabolites. Its function is to protect cells from xenobiotics and toxic compounds [23]. In particular, P-gp and MRP1 are located in the cell membrane and have a broad substrate spectrum, which is important in cancer cells. Approximately 90% of the drugs in cancer cells are substrates for this transporter [22-24]. PKC can regulate various cellular processes, such as cell proliferation, differentiation, and death [25]. It has been reported that overexpression of the PKCα isozyme can inhibit apoptosis and promote chemical resistance [8]. Therefore, compared with parental cancer cells, the expression of P-gp, MRP1 and PKC in drug-resistant cancer cells and the proliferation activity of cancer cells are significantly increased.

Our research revealed that the expression of P-gp, MRP1 and PKC in SW480/5-Fu cells was significantly higher than that in SW480 cells. MTT analysis showed that the 5-FU IC50 values of SW480/5-FU xenografts and SW480 xenografts were 42.9 μg/ml and 9.516 μg/ml, respectively. These results suggest that the SW480/5-FU xenografts in this study are reliable in vivo.

The mechanism of MDR involves the intracellular and extracellular spaces, which are related to biochemical changes in cancer cells and the tumour microenvironment, respectively [21]. Many biochemical processes associated with MDR can cause tumours to become heterogeneous and dynamic tissues and continue to evolve in an attempt to overcome structural, metabolic, and immune barriers and chemotherapy drug attacks [26]. Fibrosis associated with cancer and the reorganization of collagen fibres are conducive to cancer cell invasion [27-28]. Therefore, cancer cells benefit from this microenvironment, which reduces the action of or access to chemotherapy drugs [20], thereby promoting the development of MDR.

Changes in the microenvironment of cancer cells provide a pathophysiological basis for MR to monitor tumour resistance. DWI is currently the only method that can be used to noninvasively detect the microscopic diffusion motion of water molecules (random Brownian motion) in vivo. The movement of water molecules in biological tissues that generate DWI signals includes extracellular space diffusion, intracellular space diffusion, and intravascular space diffusion (or perfusion) [6,29].

The ADC value is obtained from at least two images with b values between 0 and 500–1000 s/mm2. The ADC value reflects water molecular diffusion [30-32] but also affects perfusion-related motion that the monoexponential model cannot explore [33-36]. Le Bihan [37] proposed the concept of IVIM (i.e., perfusion-related motion). The diffusion and perfusion effects were analysed by using a double exponential model and determining the true diffusion coefficient D, the perfusion fraction f and the pseudo diffusion coefficient D* [34]. D represents the diffusion mobility of water molecules in tissues [33,38-40]. f reflects the relative contribution of microvascular blood flow to the DWI signal, and D* depends on the blood flow velocity and the length of the microvascular segments [34,37,39].

Any factors that may shrink the extracellular compartment or alter water exchange at the cell membrane impair the diffusion of water molecules [5]. Water diffusion-limited tissues exhibit high signal intensity on DWI and low signal intensity on ADC maps. Diffusion restriction can also be quantified by calculating the ADC values in specific target regions (ROIs) [5-7]. In general, the D value has a negative correlation with cell density [40].

In the present study, analysis of tumour tissue sections showed

that cancer cells in the 5-FU-resistant group were more irregularly shaped, arranged more closely with narrower extracellular spaces, and had a smaller nucleus:cytoplasm ratio than those in the 5-FU-responsive group. Therefore, compared with 5-FU-responsive cancer tissues, the diffusion motion of water molecules into the extracellular and intracellular spaces in 5-FU-resistant tissues was inhibited. The increased expression of the ABC transporter restricts the diffusion of water molecules across membranes. Our result is in good agreement with those from previous studies [14-15], in which the ADC value of the drug-resistant group was lower than that of the drug-responsive group ($P<0.01$). The D value of 5-FU-responsive colon cancer tissue in xenografts was higher than that of 5-FU-resistant tissue ($P<0.01$) and appeared to be inversely correlated with the expression of P-g p, MRP1 and PKC. It has been reported that the D value of tumours in patients with nasopharyngeal carcinoma after chemotherapy is significantly increased, which is a sign of decreasing cellularity caused by chemotherapy drugs [41].

Our work revealed a mechanism by which D values are lower in 5-FU-resistant colon cancer tissue than in 5-FU-responsive colon cancer tissue. Colon cancer cells with 5-FU resistance have high cell turnover (with increased cell division), resulting in densely packed cells and enlarged nuclei, which prevent water molecules from diffusing. It is expected that the D value can be used to quantify tumour hypercellularity in vivo.

Concerning the other perfusion-weighted parameters f & D*, f represents the contribution of water moving in capillaries, and D* represents diffusion within the microcirculation [6]. In theory, the IVIM perfusion method offers a way to study microcirculatory blood flow properties and to monitor the early response of cancer to treatment with an anti-angiogenic or vascular targeting agent in vivo [42]. Anti-angiogenic drugs control the growth of tumours by affecting the vascular endothelial growth factor (VEGF) family pathway [43-44]. Cui et al. [45] found that f and D* were significantly reduced in mice with nasopharyngeal carcinoma 1 day after treatment with an anti-angiogenic agent compared with treatment with a control. Vascular targeting agents are designed to cause the rapid, selective closure of tumour blood vessels [46]. Joo et al. [47] found that f, D* and fD* were significantly reduced 4 hours after the administration of a vascular-disrupting agent to a rabbit model of liver cancer. Subsequent observations showed that the decrease in f and fD* at 4 hours was inversely related to the increase in tumour size on day 7 after treatment [47].

In this study, the f and D* values of the responsive colon cancer group (SW480) were higher than those of the 5-FU-resistant colon cancer group (SW480/5-FU). The difference in the D* value between the two groups was significant ($P<0.05$), but there was no significant difference in the f value between the two groups ($P>0.05$). Analysis of tumour tissue sections showed no significant difference in intratumorally necrosis between the 5-FU-responsive and 5-FU-resistant groups ($P>0.05$). These results suggest that perfusion and blood flow velocity and the length of the microvascular segments in 5-FU-resistant cancer tissue are decreased but do not cause additional ischaemic necrosis in the tumour. We speculate that 5-FU-resistant colon cancer cells have improved viability in a low perfusion state.

Ideally, a careful mechanistic verification using high-resolution small animal MRI scanners can ensure the correlation between pathological changes and MRI performance, but this is beyond the scope of the current research. To avoid the above shortcomings, colon cancer xenograft models with tumours close to 1.5 cm in size were included in this study. This reduced the sample size of the study (8 colon cancer lesions per group). Therefore, this study provides only preliminary results based on a small sample size and not a comparison of the perfusion-related parameters of IVIM with the histological micro vessel density (MVD) of cancer lesions, which should be addressed in future studies.

In conclusion, our study demonstrated that the ADC value of DWI with a single-exponential model and the diffusion coefficients D and D* of IVIM are valuable for discriminating 5-FU-responsive and 5-FU-resistant colon cancer in vivo. IVIM is expected to be a simple and practical way to quantitatively monitor tumour resistance in vivo, and the ADC, D & D* values may be used as imaging biomarkers.

6. Acknowledgements

This work was supported by the Natural Science Foundation of Guangdong (2015A030313732).

An earlier version of this manuscript has been presented as a poster in Oral Session - Diffusion in Cancer: Clinical Studies & Validation (link: https://www.ismrm.org/21/program-files/TeaserSlides/TeasersSessions/23.html) and in Digital Poster (link: https://www.ismrm.org/21/program-files/D-143.htm). We declare that this manuscript has not been submitted elsewhere.

The authors would like to acknowledge Qi-feng Pan for MRI technical assistance.

Reference

1. Sun KX, Zheng RS, Zhang SW, Zeng HM, Zou XN, Chen R, et al. Report of Cancer Incidence and Mortality in Different Areas of China, 2015. China Cancer. 2019; 28:1–11.
2. Hana J, Li J, Tang K, Zhang H, Guo B, Guo B, et al. miR-338-3p confers 5-fluorouracil resistance in p53 mutant colon cancer cells by targeting the mammalian target of rapamycin miR-338-3p.Experimental Cell Research. 2017; 360(2): 328-36.
3. Soerjomataram I, Lortet-Tieulent J, Parkin DM, Ferlay J, Mathers C, Forman D, Bray F. Global burden of cancer in 2008: a systematic analysis of disability-adjusted life-years in 12 world regions. Lancet. 2012; 380(9856): 1840–50.
4. Abdel-Rahman WM, Al-khayyal NA, Nair VA, Aravind SR, Saber-Ayad M. Role of AXL in invasion and drug resistance of co-

lon and breast cancer cells and its association with p53 Alterations. World J Gastroenterol. 2017; 23(19): 3440–8.

5. De Robertis R, Tinazzi Martini P, Demozzi E, Dal Corso F, Bassi C, Pederzoli P, et al. Diffusion-weighted imaging of pancreatic cancer. World J Radiol. 2015; 7(10): 319–28.
6. Mannelli L, Nougaret S, Vargas HA, Do RK. Advances in Diffusion-Weighted Imaging. Radiol Clin North Am. 2015; 53(3): 569–81.
7. Bae H, Yoshida S, Matsuoka Y, Nakajima H, Tanaka H, Oya M, et al. Apparent diffusion coefficient value as a biomarker reflecting morphological and biological features of prostate cancer. Int Urol Nephrol. 2014; 46(3): 555–61.
8. Higano S, Yun X, Kumabe T, Watanabe M, Mugikura S, Umetsu A, et al. Malignant astrocytic tumors: clinical importance of apparent diffusion coefficient in prediction of grade and prognosis. Radiology. 2006; 241(3): 839–46.
9. Curvo-Semedo L, Lambregts DM, Maas M, Beets GL, Caseiro-Alves F, Beets-Tan RG. Diffusion-weighted MRI in rectal cancer: apparent diffusion coefficient as a potential noninvasive marker of tumor aggressiveness. J Magn Reson Imaging. 2012; 35(6): 1365–71.
10. Nougaret S, Vargas HA, Lakhman Y, Sudre R, Do RK, Bibeau F, et al. Intravoxel incoherent motion-derived histogram metrics for assessment of response after combined chemotherapy and radiation therapy in rectal cancer: initial experience and comparison between single-section and volumetric analyses. Radiology. 2016; 280(2): 446–54.
11. Yang XY, Chen Y, Wen ZQ, Liu YY, Xiao XJ, Liang W, et al. Non-invasive MR assessment of the microstructure and microcirculation in regional lymph nodes for rectal cancer: a study of intravoxel incoherent motion imaging.Cancer Imaging. 2019; 19: 70.
12. Hu J, Yu X, Yin P, Du B, Cai X. Intravoxel Incoherent Motion Diffusion-Weighted MR Imaging for Monitoring the Immune Response of Immunogenic Chemotherapy. Front Oncol. 2022; 12: 796936.
13. Zhou B, Zhou Y, Tang Y, Bao Y, Zou L, Yao Z, et al. Intravoxel incoherent motion MRI for rectal cancer: correlation of diffusion and perfusion characteristics with clinical-pathologic factors. Acta Radiol. 2023; 64(3): 898-906.
14. Xie Q, Yang YM, Wu MY, Zhang DX, Lei ZX, Zhang J, et al. Detection of the drug resistance of human colon cancer in mice with magnetic resonance diffusion-weighted imaging. Journal of China Clinic Medical Imaging. 2016; 27: 355–8.
15. Xie Q, Wu MY, Yang YM, Zhang DX, Lei ZX, Zhang J, et al. In vivo detection of the reversal effects using rAd/p53 to human colon cancer in mice with diffusion-weighted magnetic resonance imaging. Chinese Journal of Magnetic Resonance Imaging. 2016; 7: 56–60.
16. Xie Q, Wu MY, Zhang DX, Yang YM, Wang BS, Zhang J, et al. Synergistic anticancer effect of exogenous wild-type p53 gene combined with 5-FU in human colon cancer resistant to 5-FU in vivo. World J Gastroenterol. 2016; 22(32): 7342–52.
17. Workman P, AboagyeE O, Balkwill F, Balmain A, Bruder G, Chaplin DJ, et al. Committee of the National Cancer Research Institute. Guidelines for the welfare and use of animals in cancer research. British Journal of Cancer. (2010), 102: 1555–77.
18. Yang YM, Xie Q. In vivo detection of the drug resistance of human colon cancer in mice with intravoxel incoherent motion diffusion imaging and proton magnetic resonance spectrum. Guangzhou Medical University Master Thesis (2017).
19. Bayón-Cordero L, Alkorta I, Arana L. Application of Solid Lipid Nanoparticles to Improve the Efficiency of Anticancer Drugs. Nanomaterials. 2019; 9(3): 474.
20. Kapse-Mistry S, Govender T, Srivastava R, Yergeri M. Nanodrug delivery in reversing multidrug resistance in cancer cells. Front Pharmacol. 2014; 5: 1–22.
21. Kartal-Yandim M, Adan-Gokbulut A, Baran Y. Molecular mechanisms of drug resistance and its reversal in cancer. Crit Rev Biotechnol. 2016; 36(4): 716–26.
22. Alakhova DY, Kabanov AV. Pluronics and MDR reversal: An update. Mol Pharm. 2014; 11(8): 2566–78.
23. Bugde P, Biswas R, Merien F, Lu J, Liu DX, Chen M, et al. The therapeutic potential of targeting ABC transporters to combat multi-drug resistance. Expert Opin Ther Targets. 2017; 21(5): 511–30.
24. Cavaco MC, Pereira C, Kreutzer B, Gouveia LF, Silva-Lima B, Brito AM, et al. Evading P-glycoprotein mediated-efflux chemoresistance using solid lipid nanoparticles. Eur J Pharm Biopharm. 2017; 110: 76–84.
25. Deepanwita P, Alakananda B. Protein kinase C-eta regulates Mcl-1 level via ERK1. Cell Signal. 2017; 40: 166–71.
26. Bellone M, Elia AR. Constitutive and acquired mechanisms of resistance to immune checkpoint blockade in human cancer. Cytokine Growth Factor Rev. 2017; 36: 7–24.
27. Alfano M, Nebuloni M, Allevi R, Zerbi P, Longhi E, Lucianò R, et al. Linearized texture of three-dimensional extracellular matrix is mandatory for bladder cancer cell invasion. Scientific reports. 2016; *6*: 36128.
28. Nebuloni M, Albarello L, Andolfo A, Magagnotti C, Genovese L, Locatelli I, et al. Insight On Colorectal Carcinoma Infiltration by Studying Perilesional Extracellular Matrix. Scientific reports. 2016; *6*, 22522.
29. Dixon WT. Separation of diffusion and perfusion in intravoxel incoherent motion MR imaging: a modest proposal with tremendous potential. Radiology. 1988; 168(2): 566–7.
30. Parikh T, Drew SJ, Lee VS, Wong S, Hecht EM, Babb JS, et al. Focal liver lesion detection and characterization with diffusion-weighted MR imaging: comparison with standard breath-hold T2-weighted imaging. Radiology. 2008; 246(3): 812–22.
31. Gourtsoyianni S, Papanikolaou N, Yarmenitis S, Maris T, Karantanas A, Gourtsoyiannis N. Respiratory gated diffusion-weighted imaging of the liver: value of apparent diffusion coefficient measurements in the differentiation between most commonly encountered benign and malignant focal liver lesions. Eur Radiol. 2008; 18(3): 486–92.
32. Coenegrachts K, Delanote J, Ter Beek L, Haspeslagh M, Bipat S,Stoker J, Van Kerkhove F, et al. Improved focal liver lesion detection: comparison of single-shot diffusion-weighted echoplanar and single-shot T2 weighted turbo spin echo techniques. Br J Radiol. 2007; 80(995): 524–31.

33. Padhani AR, Liu G, Koh DM, Chenevert TL, Thoeny HC, Takahara T, et al. Diffusion-weighted magnetic resonance imaging as a cancer biomarker: consensus and recommendations. Neoplasia. 2009; 11(2): 102–25.
34. Koh DM, Collins DJ, Orton MR. Intravoxel incoherent motion in body diffusion-weighted MRI: reality and challenges. Am J Roentgenol. 2011; 196: 1351–61.
35. Guiu B, Cercueil JP. Liver diffusion-weighted MR imaging:the tower of Babel? Eur Radiol. 2011; 21(3): 463–7.
36. Murtz P, Sprinkart AM, Reick M, Pieper CC, Schievelkamp AH, König R, et al. Accurate IVIM model-based liver lesion characterisation can be achieved with only three b-value DWI. Eur Radiol. 2018; 28(10): 4418-28.
37. Le Bihan D, Breton E, Lallemand D, Aubin ML, Vignaud J, Laval-Jeantet M. Separation of diffusion and perfusion in intravoxel incoherent motion MR imaging. Radiology. 1988; 168(2): 497–505.
38. Taouli B, Koh DM. Diffusion-weighted MR imaging of the liver. Radiology. 2010; 254(1): 47–66.
39. Takahara T, Kwee TC. Low b-value diffusion-weighted imaging:emerging applications in the body. J Magn Reson Imaging. 2012; 35(6): 1266–73.
40. Aoyagi T, Shuto K, Okazumi S, Hayano K, Satoh A, Saitoh H, et al. Apparent diffusion coefficient correlation with oesophageal tumour stroma and angiogenesis. Eur Radiol. 2012; 22(6): 1172–77.
41. Noij DP, Martens RM, Marcus JT, de Bree R, Leemans CR, Castelijns JA, et al. Intravoxel incoherent motion magnetic resonance imaging in head and neck cancer: A systematic review of the diagnostic and prognostic value. Oral Oncology. 2017; 68: 81–91.
42. Federau C. Intravoxel incoherent motion MRI as a means to measure in vivo perfusion: A review of the evidence. NMR in biomedicine. 2017; *30*(11).
43. Folkman J. Tumor angiogenesis: therapeutic implications. N Engl J Med. 1971; 285(21): 1182–6.
44. Ferrara N, Kerbel RS. Angiogenesis as a therapeutic target. Nature. 2005; 438(7070): 967-74.
45. Cui Y, Zhang C, Li X, Liu H, Yin B, Xu T, et al. Intravoxel Incoherent Motion Diffusion-weighted Magnetic Resonance Imaging for Monitoring the Early Response to ZD6474 from Nasopharyngeal Carcinoma in Nude Mouse. Sci Rep. 2015; 5:16389.
46. Thorpe PE. Vascular targeting agents as cancer therapeutics. Clin Cancer Res. 2004; 10(2): 415–27.
47. Joo I, Lee JM, Han JK, Choi BI. Intravoxel incoherent motion diffusion-weighted MR imaging for monitoring the therapeutic efficacy of the vascular disrupting agent CKD-516 in rabbit VX2 liver tumors. Radiology. 2014; 272: 417–26.